"Biomechanics of Superparamagnetic Nanoparticles for Laser Hyperthermia"

Maryam Fatima[a], Ayesha Sohail[a*], Khush Bakhat Akram[b],
Lubna Sherin[c], Saad Ihsan Butt [a], M. Abid [d] *and* O. Anwar Bég [e]

[a]*Department of Mathematics, Comsats University Islamabad, Lahore Campus 54000, Pakistan*
[b]* National University of Technology, NUTECH, Islamabad, Pakistan*
[c]*Department of Chemistry, Comsats University Islamabad, Lahore Campus, 54000, Pakistan*
[d]*Interdisciplinary Research, Comsats University Islamabad, Wah Cantt Campus, 54000, Pakistan*
[e]*Department of Aeronautical/Mechanical Engineering, University of Salford, Manchester, M5WT, UK*

Abstract:
Nanoparticle hyperthermia treatment is progressing with the passage of time, and with the development in the field of hybrid nanoparticles synthesis. The transient heat transfer in magnetite-graphene nanocomposite in three-dimensions under conduction is studied in this this research. The proposed model is simulated in a finite element solver framework. Novel hybrid nanoparticles were synthesized. Their chemical properties and their heat transfer properties were examined. By mathematical modelling results, the effective hybrid nanoparticle is chosen that can be used as a drug in hyperthermia process. Current developments in nanotechnology have improved the ability to precisely modify the features and properties of MNPs for these biomedical applications. The accurate control on the magnetic properties of the particle is the key in hyperthermia applications. By these magnetic particles, the desired temperature can be achieved for laser hyperthermia. In this article, a detailed investigation is reported for understanding the properties and novelty of the new nanoparticles. The merits and demerits of synthesized hybrid nanoparticles are also discussed with regard to whether the nanocomposites can be implemented as a drug or not.

Keywords: Nanohyperthermia, Laser thermal therapy, Heating enhancer

1 Introduction:

Superparamagnetic nanoparticles have been widely used in medical research because of their unusual magnetic properties and biocompatibility. Investigation on superparamagnetic nanoparticles has been deeply accomplished in drug delivery, chemotherapy, hormonal therapy, radiation therapy, hyperthermia therapy, medical imaging and targeting cancer treatment [1-5]. Cancer is also known as a malignancy which is essentially

the abnormal growth of cells. Cancer is the second leading cause of death world wide and it is responsible for an estimated 9.6 million deaths in 2018. Cancer can be cured by hyperthermia treatment by using superparamagnetic nanoparticles with the aid of external alternating magnetic field [6], radiotherapy [7] and by laser [8]. Cancer thermotherapy is a method of cancer treatment where cancer cells are killed by flaunting the body tissues to high temperatures. Common approaches of cancer treatment such as old-fashioned surgery method, radiation therapy, chemotherapy, tumor thermotherapy has been shown to have some side effects during and after treatment [7]. That's why thermotherapy has been widely acknowledged. During hyperthermia treatments, the measurement of the actual temperature distribution in the tumour or immediately adjacent tissue is crucially important to the clinical evaluation of the quality of hyperthermia. In this process, the variety of the target tissues temperature have great influences and effectiveness on body. Moreover, in this procedure heat circulates from the target tissue to the surroundings which causes heat injury to normal tissues. Toxicity of hyperthermia in generally is low. The incidence of (reversible) pain at the treated region varies between $0\pm60\%$. Burns are a typical hyperthermia associated toxicity with low incidence, that are dependent on correct heating techniques. The combination of local or interstitial hyperthermia with radiotherapy resulted in tissue damage that was not significantly greater than that in radiotherapy-sites alone .

Latest innovation of hyperthermia therapy is implification of lasers, which can be used to control the heating effect in body. Lasers have very effective properties which can help for heat cause. Laser can emit light with high intensity and it is extremely directional,self-coloured, and coherent. Wavelength range for visible to infrared light is from 400nm to 900nm. The penetrability of light in living tissue increases with the wavelength [9]. When the laser beam reaches to tissues, the heat is first act on the surface of the tissues that are open to the irradiation directly and then slowly spreads to the surrounding of tissues [10]. This allows continuous heating of the tumor area. Moreover, by regulating the output power of infrared laser instrument the temperature of hyperthermia procedure can easily be controlled. Because of simple operation and low cost and efficient infrared laser is an ideal heat source for tumor hyperthermia. Magnetic nanoparticles have great importance in laser hyperthermia. Laser's heat circulation have different effects with different superparamagnetic nanoparticles. The heating process is completely induced in the magnetic nanoparticles under alternating magnetic field due to Neel relaxation and Brownian relaxation losses. As there is reduced blood flow in tumor area, containing disorganized blood vessels, the heat dissipation to surrounding area is limited. Therefore, cancer cells are more susceptible for apoptosis at relatively mild heating up to 315.15K (42^oC) as compared to healthy cells. Literature shows that a temperature range of 314.95K - 317.15K (41.8-44^oC) is most suitable for the entire body hyperthermia [11].

During this research we have focused on novel nanoparticles. Due to biocompatibility and strong inherent magnetic properties, Fe_3O_4 and synthesized nanohybrids were used using it. Fe_3O_4 nanoparticles have strong anisotropic dipolar interactions which causes agglomeration and precipitation, due to which their colloidal solubility is lost, and their activity is reduced, making them vulnerable.

Therefore, it is challenging to incorporate Fe_3O_4 nanoparticles in both in-vitro and in-vivo experiments.To prevent their agglomeration and precipitation, we have developed a support of reduced graphene oxide sheets, for making Fe_3O_4 nanoparticles immobilized. In this work, thermal reduction method has been used for producing graphene and Fe_3O_4-

graphene nanohybrids. Graphene has gained attention for tremendous applications. Large thermal conductivity of graphene ($\kappa \sim 5.3 \times 10^3$ Wm^{-1}) [12], high exibility and strength (elastic stiffness ~ 340 Nm^{-1}, Youngs modulus ~ 1.0 TPa , and breaking strength ~ 42 Nm^{-1}) [13, 14]and excellent biocompatibility lead to remarkable properties for the development of prototype devices for biological applications. From all the temperature measurements gained as temperature vs. time and time-averaged temperatures can be calculated at each monitored site.

2 Materials and Method:

2.1 Materials:

For synthesis of Fe$_3$O$_4$-graphene nanohybrids the high quality of expandable graphite powder of mean size 25 μm (purity 99.99%), FeCl$_3$.6H$_2$O (purity 99%), FeCl$_2$.4H$_2$O (purity 99.8%),HCl , KMnO$_4$(purity 99%), 32% NH$_3$ solution and high grade H$_2$SO$_4$ and H$_2$O$_2$ (30 wt.). All reactions were carried out using deionized (DI) water. Firstly, Graphene Oxide was synthesized using graphite powder by modified Hummers method [15]. 5g graphite powder was added in 125 mL H$_2$SO$_4$ at 0°C by continuous mixing to avoid agglomeration.Once the powder was well dispersed, 15g KMnO$_4$ was added to the mixture slowly, keeping the temperature below 15°C. Gradually the mixture was brought to room temperature [16].150 ml of DI water was added slowly to the mixture to dilute it after which mixture was washed out and dried at room temperature and Grey colored GO powder remained. Magnetite- graphene oxide F$_x$G$_{100x}$ compositions have been synthesized, where x=(0, 25, 45, 65, 75, 85, 100) refers to the weight percentage of magnetite in the nanohybrid. Note that, the composition with x=0 specifies pure graphene and x=100 specifies pure magnetite. Appropriate amounts of FeCl$_3$.6H$_2$O and FeCl$_2$.4H$_2$O and graphene oxide (GO) were weighed for each composition. After the procedure sample were named according to the weight % ratio in the compositional formula F$_x$G$_{100x}$ (x = 0, 25, 45, 65, 75, 85, 100) as G, F$_{25}$G$_{75}$, F$_{45}$G$_{55}$, F$_{65}$G$_{35}$, F$_{75}$G$_{25}$, F$_{85}$G$_{15}$ and F respectively. For example, F$_{75}$G$_{25}$ refers to the hybrid containing 75 wt. % magnetite and 25 wt.% graphene.

2.2 Mathematical Model:

In this model, Laser beam is used for heat transfer in various substrates. Basically, the laser beam acts as a heat source. For hyperthermia process laser is used for heat transfer at subjected area to kill cancer cell. A model is proposed where G, F$_{25}$G$_{75}$, F$_{45}$G$_{55}$, F$_{65}$G$_{35}$, F$_{75}$G$_{25}$, F$_{85}$G$_{15}$ and Fe used as a substrate one by one. Laser beam is moving over a surface to produce the required localized heating. In this case, each layer of substrate is very thin. The localized transient heating was generated by a laser beam, which was moving in a circular path over the substrate. Beam's penetration's depth can be described by an absorption coefficient k$_{abs}$, which depends on the ambient temperature. From this model, the penetration depth and the temperature distribution is understandable. The substrate is formed as a three dimensional object with 1mm thickness and 10mm-by-10mm width. It manages the variation of laser intensity with penetration depth using one dimensional geometry that represents the substrates thickness. The model is formed by transient heat

transfer in 3-D geometry by conduction. The transient energy transport equation for heat conduction is:

$$\rho C_p \frac{\partial T}{\partial t} + \nabla \cdot (-\underline{k}\nabla T) = \zeta \tag{1}$$

Here ρ is the density with unit kg/m^3, C_p is the specific heat capacity with unit J/(kg.K), $\underline{k}$ is the thermal conductivity tensor and ζ is the heat source which is zero over here. The material properties of substrates are derived an anisotropic conductivity of $\kappa=(\mathrm{k}_{xx},\mathrm{k}_{yy},\mathrm{k}_{zz})$ with unit W/((m.K)). For the model, an assuption of insulated boundries is made. In 1-D geometry,the weak form, subdomain application mode is used to model the laser penetration. The equation which describes the laser penetration is:

$$\frac{\partial I}{\partial \acute{x}} = -k_{abs}I \tag{2}$$

I represents the relative laser intensity, $\acute{x}$ represents the 1-D coordinate, and k$_{abs}$ is the absorption coefficient. The absorption coefficient can depend on the temperature which is:

$$k_{abs} = 8 \cdot 10^3 m^{-1} - 10(m.K)^{-1}(T - 300K) \tag{3}$$

The volumetric heat source term ζ in the 3-D geometry is:

$$\zeta = P_{in}k_{abs}I \tag{4}$$

where P$_{in}$ is the total power of the incoming laser beam. Both of these equations are included in the Weak Form, Subdomain application mode, where they work as a equation, which is given as :

$$I_{test}(I_x - k_{abs}I) + k_{abs}I P_{in}T_{test} \tag{5}$$

The first part of this expression describes the penetration equation, and the second part comes from the heat-source term in the 3-D Heat Transfer application mode. At the left boundary, homogeneous Neumann condition is applied and at the right boundary the relative intensity I is equal to unity. The total incoming laser power P$_{in}$ is 50 W. The model implements the heat source's motion when we coupled the 3-D temperature variable T to the 1-D equation. It does so with a subdomain extrusion coupling variable using a general transformation. A time-dependent transformation expression results in a moving heat source. This case describes a circular repeating motion using the transformation expressions.

$x = c\sin(\omega t)$
$y = c\cos(\omega t)$
$z = \acute{x}$

where x,y and z are 3-D coordinates and $\acute{x}$ represents the 1-D coordinate. c is the radius of circular motion , ω is the angular velocity and t is time. The parameter values used in model are c = 0.02m and ω = 10 rad/s. For the laser motion the roughly time period is [0,1] sec. The 3-D model is formed by using an extruded triangular mesh, which has a fine resolution close to the laser incident line and is coarse elsewhere. This results in a high-resolution solution with minimum computation requirements.From the schematic diagram, we can see the location of laser beam (i.e. the hotspot). Here the laser beam moves from right to left, and the warm side is on the right side of the peak. The temperature reaches at different points according to the substrate. The substrate types which used in model are explained in table (see table 6). Mathematical model is shown in figure (see figure 6)

3 Results:

Different materials will be taken one by one so nanoparticle's heat flux variation and temperature changes can be understand. Because heat pays an important role in hyperthermia. These model can help us to understand that which nanoparticle is more effective in laser hyperthermia process and which nanoparticle is harmful for human being.

3.1 Iron(Fe) as a substrate:

Ferrous metals have a high carbon content which generally makes them vulnerable to rust when exposed to moisture. They have magnetic properties. Fe have 3.4 W/mk thermal conductivity, density 5150kg/m^3 and heat capacity C_p 940 J/kgK. In figure 2 variation of time is 0.08s, 0.48s, 0.86 and 1s which shows that time is the most important parameter in this model. At t=0.08s the stream lines shows the heat flux and the temperature varies from 300K to 500K. At t=0.46s, temperature varies from 350K to 550K. At t=0.86s, temperature varies from 400K to 600K. At t=1s, temperature varies from 300K 700K. We have presented these results in figure 2.

3.2 $F_{25}G_{75}$ as a substrate:

In figure 3, $F_{25}G_{75}$ is used as a drug. By changing the concentration of atoms , heat transfer effect will be definitely changes. It is understood that changes occurs with respect to time. At t=0.08s, streamlines shows the heat flux changes and temperature varies between 300K to 306K. At t=0.46s, temperature varies between 300.034K to 307K. At t=0.86s, temperature varies between 300.311K to 312K. At t=1s, temperature varies between 300.441K to 310K.

3.3 $F_{45}G_{55}$ as a substrate:

In figure 4, $F_{45}G_{55}$ is used as a substrate. With respect to time temperature increases as shown in figure. At t=0.08s, streamlines shows the heat flux changes and minimum temperature is 299.997K and maximum temperature is 308.5K. At t=0.46s, minimum temperature is 300.008K and maximum temperature is 309.249K. At t=0.86s, minimum temperature is 300.152K and maximum temperature is 315.874K. At t=1s, minimum temperature is 300.254K and maximum temperature is 313.359K.

3.4 $F_{65}G_{35}$ as a substrate:

In figure 5, $F_{65}G_{35}$ is used as a substrate. With respect to time temperature increases as shown in figure. At t=0.08s, streamlines shows the heat flux changes and minimum temperature is 299.995K and maximum temperature is 310K. At t=0.46s, minimum temperature is 299.997K and maximum temperature is 312K. At t=0.86s, minimum temperature is 300.025K and maximum temperature is 314K. At t=1s, minimum temperature is 300.069K and maximum temperature is 318.243K.

3.5 $F_{75}G_{25}$ as a substrate:

In figure 6, $F_{75}G_{25}$ is used as a substrate. With respect to time temperature increases as shown in figure. At t=0.08s, streamlines shows the heat flux changes like in the above figures. Minimum temperature is 299.988K and maximum temperature is 312K. At t=0.46s, minimum temperature is 299.996K and maximum temperature is 315K. At t=0.86s, minimum temperature is 300K and maximum temperature is 318K. At t=1s, minimum temperature is 300.008K and maximum temperature is 320K.

3.6 $F_{85}G_{15}$ as a substrate:

In figure 7, $F_{85}G_{15}$ is used as a substrate. With respect to time temperature increases as shown in figure. At t=0.08s, streamlines shows the heat flux changes and minimum temperature is 299.953K and maximum temperature is 310K. At t=0.46s, minimum temperature is 299.966K and maximum temperature is 315K. At t=0.86s, minimum temperature is 299.979K and maximum temperature is 320K. At t=1s, minimum temperature is 299.989K and maximum temperature is 325K.

3.7 Graphene(G) as a substrate:

In figure 8, Graphene is used as a substrate. With respect to time temperature increases as shown in figure. At t=0.08s, streamlines shows the heat flux changes and minimum temperature is 300.045K and maximum temperature is 306K. At t=0.46s, minimum temperature is 302.943K and maximum temperature is 311.838K. At t=0.86s, minimum temperature is 306.65K and maximum temperature is 316K. At t=1s, minimum temperature is 307.93K and maximum temperature is 318.227K.

4 Discussion:

During this research, we have considered special type of nanoparticles. In the recent literature, studies are available, such as the research group led by Frazi et'al [17], provided a documented proof, where the significance of nanoparticles (such as magnetite-graphene nanocomposite), for biological applications was verified. In this article the physical properties of the particles were incorporated with a mathematical model. Mathematical results verfieid that Fe can never be used as a drug in laser hyperthermia because maximum temperature which is gained is 700K, that can burn the whole body easily. However, Fe have magnetic properties but it exceeds the limitation of heat flux needed in hyperthermia treatment. In this study, $F_{25}G_{75}$ was the second substrate which was observed. From the mathematically observation it is shown that $F_{25}G_{75}$ can be used as drug in laser hyperthermia. In hyperthermia body temperature's range is 314.95K to 317.15K [18], so $F_{25}G_{75}$ is not harmful for human body. It did not cross the limit of heat flux needed in laser hyperthermia which is acceptable. From heat transfer streamlines and the maximum temperature of $F_{45}G_{55}$ which is approximately 316K, it is proven mathematically that it can be the perfect choice of drug in laser hyperthermia to kill cancer cells. This hybrid nanoparticles have no demerits with respect to heat flux, it's not harmful for human body. By exploring the properties of $F_{65}G_{35}$, the maximum temperature obtained is 318.243K.

That is very inappropriate for human body because it can burn it due to high temperature. From these results, this hybrid nanoparticle is not suitable for laser hyperthermia treatment. $F_{75}G_{25}$ also created a great amount of heat and gained the maximum temperature which is 320K. It exceed the limitation of human body for heat transfer. It can burn the human body which is the biggest drawback of this hybrid nanoparticle. With mathematically it's been prove that $F_{85}G_{15}$ gained maximum temperature which is 325K. That can never be the choice of drug for laser hyperthermia. Similarly, Graphene can never be treated as a drug in laser hyperthermia. It gained 318.227K, which is harmful for human body. From table 2, 3 all maximum and minimum values of temperature gained with variation of time the magnetic nano hybrid particles are discussed. From these mathematical results, the merits and demerits of synthesised magnetic nanoparticles are discussed.

5   Conclusion:

The expansion of MNPs has been significantly enhanced in the past decade by advances in nanotechnology, molecular cell biology, imaging instruments and cancer treatment. Nanoparticles of various shapes which have strong photothermal effects. Plethora of preparation of magnetic nano particles have been established to identify and treat diseases such as tumor treatment by laser-induced hyperthermia. The synthesized hybrid nano particles have very compatible properties for this therapy. In this work, this is observed that by changing the ratio of particles, different results are obtained. This study can be used in tumor therapy. Some hybrid nanoparticles have great qualities with respect to heat transfer which can show that those particles can easily used in laser hyperthermia treatment. However, some hybrid nanoparticles were harmful for human body. Hence, those particles are not good choice of drug for laser hyperthermia. With respect to stages of tumor cells magnetic nanohybrid particle can be choose as drug. The photothermal effect of magnetite-graphene nanocomposite may be well utilized as an efficient strategy in clinical cancer therapies.

6   Acknowledgement

References

[1] Sudhakar, Akulapalli,History of Cancer, Ancient and Modern Treatment Methods, *J Cancer Sci Ther*, **1**:1, 2009.

[2] Zhang L, Xue H, Gao C, Carr L, Wang J, Chu B, Jiang S, Imaging and cell targeting characteristics of magnetic nanoparticles modified by a functionalizable zwitterionic polymer with adhesive 3, 4-dihydroxyphenyl-l-alanine linkages, *Biomaterials* **31**:6582, 2010.

[3] Laurent S, Mahmoudi M, Superparamagnetic iron oxide nanoparticles, promises for diagnosis and treatment of cancer, *Int J Mol Epidemiol Genet.* **2**:367, 2011.

[4] Lee JH, Jang JT, Choi JS, Moon SH, Noh SH, Kim JW, Kim JG, Kim IS, Park KI, Cheon J, Exchange-coupled magnetic nanoparticles for efficient heat induction, *Nat Nanotechnol.Nat Nanotechnol.* **6**:418, 2011.

[5] Yang HW, Hua MY, Liu HL, Huang CY, Tsai RY, Lu YJ, Chen JY, Tang HJ, Hsien HY, Chang YS, Yen TC, Self-protecting core-shell magnetic nanoparticles for targeted, traceable, long half-life delivery of BCNU to gliomas, *Biomaterials* **32**:6523, 2011.

[6] Rosensweig RE, Heating magnetic fluid with alternating magnetic field, *J Magn Magn Mater.* **252**:370, 2002.

[7] Moroz P, Jones SK, Gray BN, Status of hyperthermia in the treatment of advanced liver cancer, *J Surg Oncol* **77**:259, 2001.

[8] Chu M, Shao Y, Peng J, Dai X, Li H, Wu Q, Shi D, Near-infrared laser light mediated cancer therapy by photothermal effect of Fe_3O_4 magnetic nanoparticles, *Biomaterials* **34**:4078, 2013.

[9] Wei HJ, Xing D, Wu GY, Jin Y, Gu HM, Optical properties of human normal small intestine tissue determined by Kubelka-Munk method in vitro, *World J Gastroenterol.* **9**:2068, 2003.

[10] Steger AC, Lees WR, Walmsley K, Bown SG, Interstitial laser hyperthermia: a new approach to local destruction of tumours, *Bmj* **299**:362, 1989.

[11] Glckl G, Hergt R, Zeisberger M, Dutz S, Nagel S, Weitschies W, The effect of field parameters, nanoparticle properties and immobilization on the specific heating power in magnetic particle hyperthermia, *J Phys Condens Matter* **18**:S2935, 2006.

[12] Balandin AA, Ghosh S, Bao W, Calizo I, Teweldebrhan D, Miao F, Lau CN, Superior thermal conductivity of single-layer graphene, *Nano Lett.* **8**:902, 2008.

[13] Neto AC, Guinea F, Peres NM, Novoselov KS, Geim AK, The electronic properties of graphene *Rev Mod Phys* **81**:109, 2009.

[14] Wan W, Zhao Z, Hu H, Gogotsi Y, Qiu J, Highly controllable and green reduction of graphene oxide to flexible graphene film with high strength, *Mater. Res. Bull.* **48**:4797, 2013.

[15] Yao Y, Miao S, Liu S, Ma LP, Sun H, Wang S, Synthesis, characterization, and adsorption properties of magnetic Fe_3O_4 @ graphene nanocomposite, *Chem. Eng. Trans.* **184**:326, 2012.

[16] Marcano DC, Kosynkin DV, Berlin JM, Sinitskii A, Sun Z, Slesarev A, Alemany LB, Lu W, Tour JM, Improved synthesis of graphene oxide, *ACS nano* 4:4806, 2010.

[17] Farazi R, Vaezi M R Molaei, M J Saeidifar, M Behnam-Ghader, Effect of pH and temperature on doxorubicin hydrochloride release from magnetite/graphene oxide nanocomposites. *Materials Today: Proceedings*, **5(7)**: 15726, 2018.

[18] Thiesen B, Jordan A, Clinical applications of magnetic nanoparticles for hyperthermia, *Int J Hyperthermia.* **24**:467, 2008.
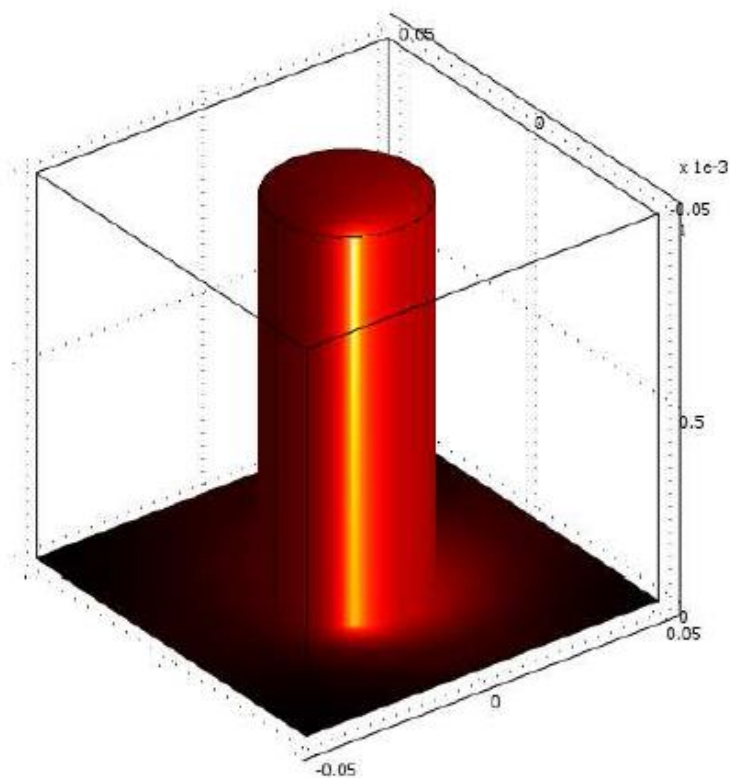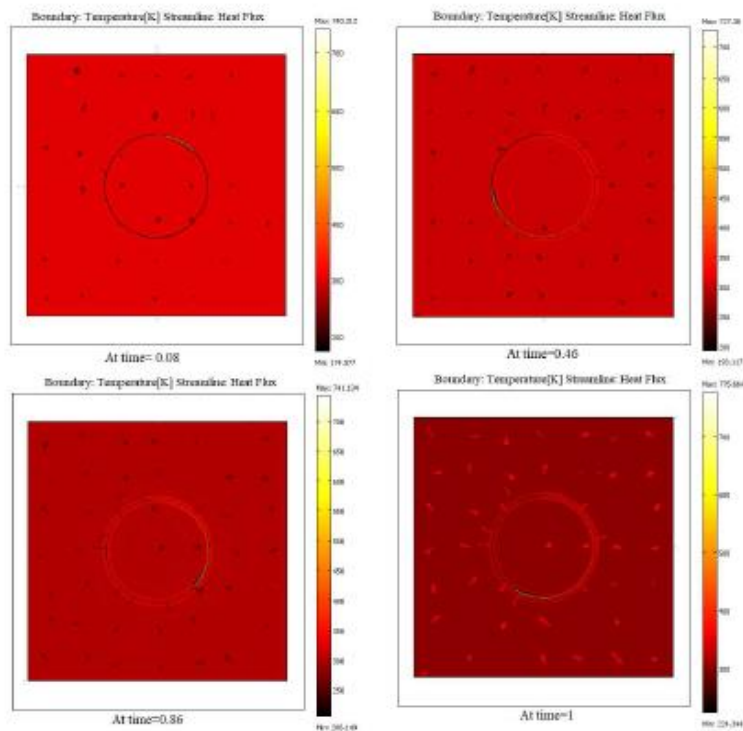
Figure 1: Model

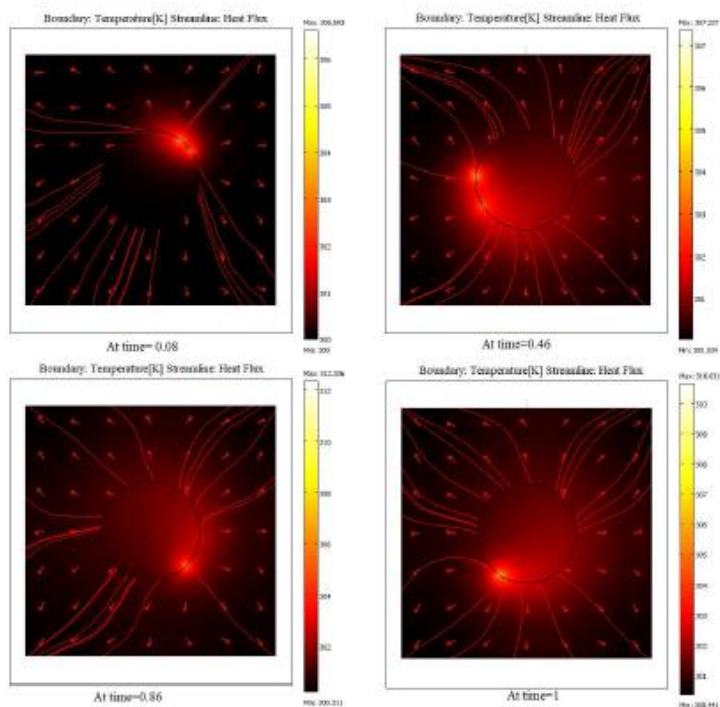Figure 2: Heat transfer:when Fe used as a substrate

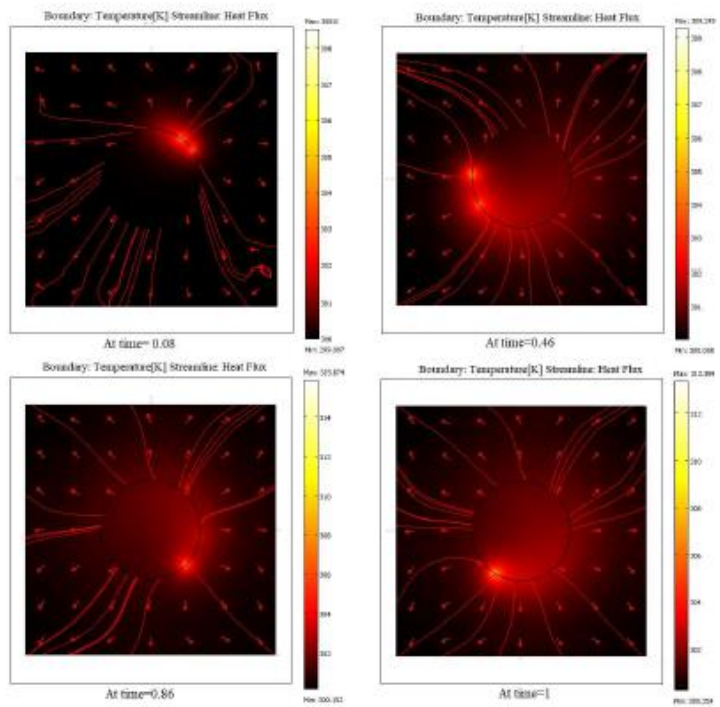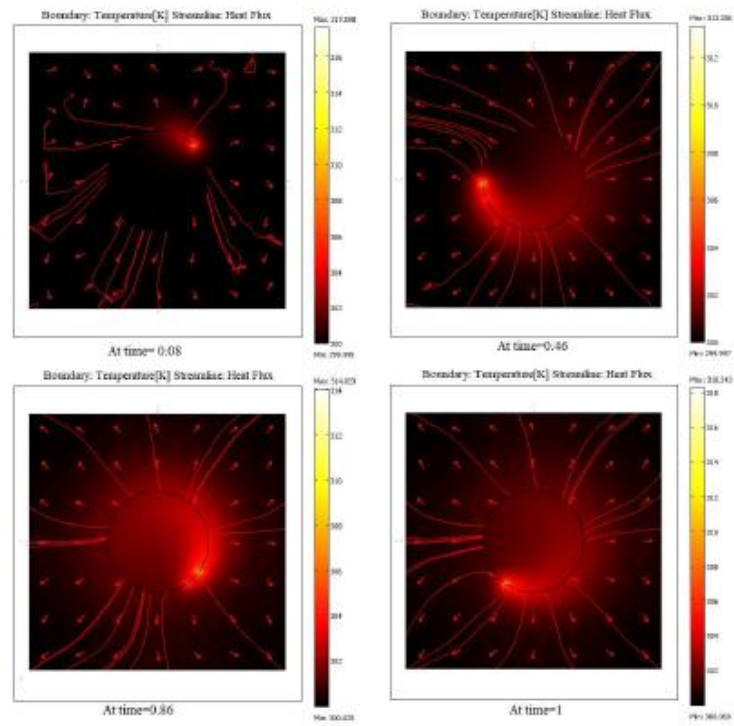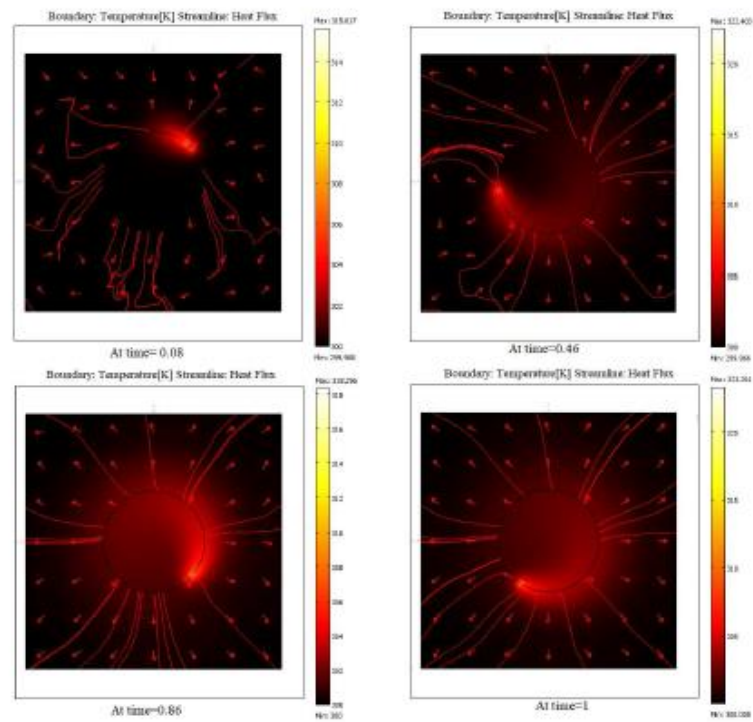Figure 3: Heat transfer:when $F_{25}G_{75}$ used as a substrate

Figure 4: Heat transfer:when $F_{45}G_{55}$ as a substrate

Figure 5: Heat transfer:when $F_{65}G_{35}$ as a substrate

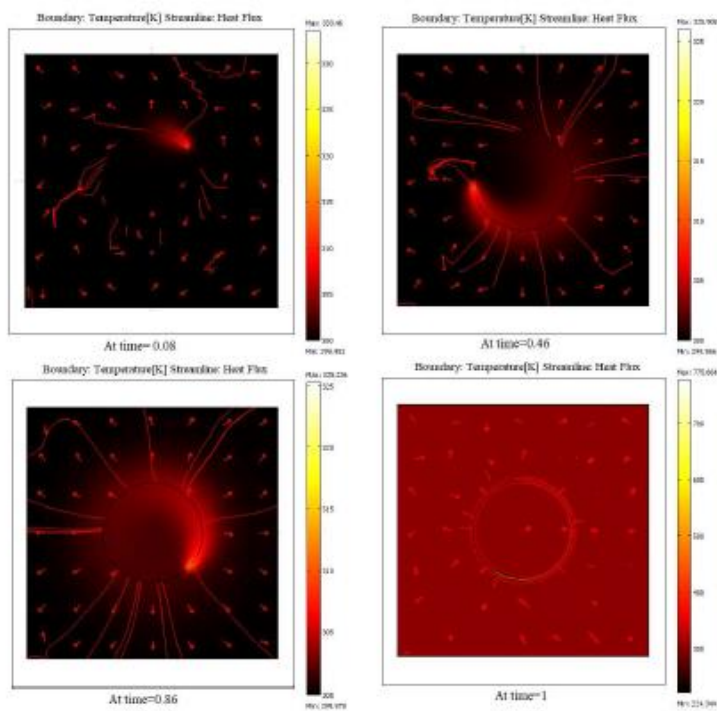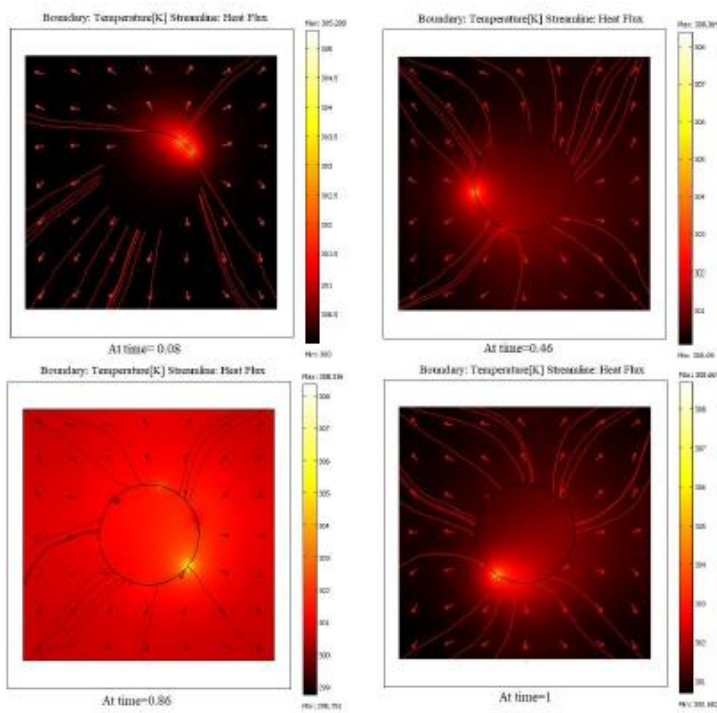Figure 6: Heat transfer:when $F_{75}G_{25}$ as a substrate

Figure 7: Heat transfer:when $F_{85}G_{15}$ as a substrate

Figure 8: Heat transfer:when graphene as a substrate

Table 1: substrates and their properties

Substrate	G	$F_{85}G_{15}$	$F_{75}G_{25}$	$F_{65}G_{35}$	$F_{45}G_{55}$	$F_{25}G_{75}$	Fe
κ	5300	802.8	1335.8	1868.8	2934.7	4000.6	3.4
ρ	2200	4700	4400	4100	3500	2900	5150
C_p	1960	1093	1195	1297	1501	1705	940

Table 2: substrate's minimum temperature with variation in time

compound	minimum temperature	$t_o=0.08$	$t_1=0.46$	$t_2=0.86$	$t_3=1$
Fe	T	300	350	400	300
	T'	—	131.58	125	-714.285
$F_{25}G_{75}$	T	300	302.034	300.311	300.441
	T'	—	0.08	0.69	0.92
$F_{45}G_{55}$	T	299.997	300.008	300.152	300.254
	T'	—	0.0289	0.36	0.72
$F_{65}G_{35}$	T	299.995	299.997	300.025	300.069
	T'	—	0.0052	0.07	0.314
$F_{75}G_{25}$	T	299.988	299.996	300	300.008
	T'	—	0.021	0.01	0.057
$F_{85}G_{15}$	T	299.953	299.966		299.989
	T'	—	0.579	0.0325	0.0714
G	T	300	300.09	302	300.682
	T'	—	-0.23	4.775	-9.414

Table 3: substrate's maximum temperature with variation in time

compound	maximum temperature	$t_o=0.08$	$t_1=0.46$	$t_2=0.86$	$t_3=1$
Fe	T	500	550	600	700
	T'	—	131.57	125	714.28
$F_{25}G_{75}$	T	306	307	312	310
	T'	—	2.63	12.5	-14.28
$F_{45}G_{55}$	T	308.5	309.249	315.874	313.359
	T'	—	1.971	16.56	-17.96
$F_{65}G_{35}$	T	310	312	314	318.243
	T'	—	5.26	5	30.3
$F_{75}G_{25}$	T	312	315	318	320
	T'	—	7.89	7.5	14.28
$F_{85}G_{15}$	T	310	315	320	325
	T'	—	13.15	12.5	35.7
G	T	304.5	305	308	308.667
	T'	—	1.32	7.5	4.76